Chin. Geogra. Sci. 2022 Vol. 32 No. 1 pp. 155−173
https://doi.org/10.1007/s11769-021-1249-x

Springer Science Press
www.springerlink.com/content/1002-0063

Characteristics and Cause Analysis of Variations in Light Precipitation Events in the Central and Eastern Tibetan Plateau, China, During 1961–2019

LI Kaifang[1], CAO Liguo[1], ZHOU Zhengchao[1], JIAO Lei[1], WANG Ning[1], LIU Ruohan[2]

(1. *School of Geography and Tourism*, *Shaanxi Normal University*, *Xi'an* 710119, *China*; 2. *School of Urban and Rural Planning and Architectural Engineering*, *Shangluo University*, *Shangluo* 726000, *China*)

Abstract: The Tibetan Plateau (TP) is one of the most sensitive areas and is more susceptible to climate change than other regions in China. The TP also experiences extremely frequent light precipitation events compared to precipitation of other intensities. However, the definition, influencing factors, and characteristics of light precipitation in the TP have not been accurately explained. This study investigated the variation characteristics of light precipitation with intensities (*Pre*) of 0.1–10.0 mm/d based on climate data from 53 meteorological stations over the central and eastern TP from 1961 to 2019. For detailed analysis, light precipitation events were classified into five grades: G1 [0.1–2.0 mm/d), G2 [2.0–4.0 mm/d), G3 [4.0–6.0 mm/d), G4 [6.0–8.0 mm/d), and G5 [8.0–10.0 mm/d). The results showed that both the amount of precipitation and number of precipitation days had increased significantly at rates of 4.0–6.0 mm/10 yr and 2.0–4.0 d/10 yr, respectively, and most precipitation events were of low intensity ($0.1 \leq Pre < 2.0$ mm/d). Light precipitation events mainly occurred in the southeast of the study area, and it showed an increasing trend from the northwest to the southeast . Abrupt changes in light precipitation primarily occurred in the 1980s. A comprehensive time series analysis using the Mann-Kendall test and Morlet wavelet was performed to characterize the abrupt changes and cycles of light precipitation. During the study period, the main periods of light precipitation corresponded to the 6 yr cycle, with obvious periodic oscillation characteristics, and this cycle coexisted with cycles of other scales. Significant correlations were observed between the amount of light precipitation and temperature over the study area. The findings will enhance our understanding of changes in light precipitation in the TP and provide Scientific basis for the definition of light precipitation in the future.

Keywords: light precipitation events; spatio-temporal variation; period analysis; Tibetan Plateau

Citation: LI Kaifang, CAO Liguo, ZHOU Zhengchao, JIAO Lei, WANG Ning, LIU Ruohan, 2022. Characteristics and Cause Analysis of Variations in Light Precipitation Events in the Central and Eastern Tibetan Plateau, China, During 1961–2019. *Chinese Geographical Science*, 32(1): 155−173. https://doi.org/10.1007/s11769-021-1249-x

1 Introduction

According to the Intergovernmental Panel on Climate Change (IPCC) Fifth Assessment Report (AR5), global warming introduces anomalies in the climate system and consequently leads to extreme climates (IPCC, 2013). Over the past century, extreme climate events have increased in frequency and severity globally, and extensive studies mainly focused on extreme climate events, including extreme droughts (Chen and Sun, 2019; An-

Received date: 2021-01-04; accepted date: 2021-02-26

Foundation item: Under the auspices of the Second Tibetan Plateau Scientific Expedition and Research Program (STEP) (No. 2019QZKK040), Key Technologies Research and Development Program of Shaanxi Province (No. 2021ZDLSF05-02), The National Natural Science Foundation of China (No. 42072208, 42101100, 41901129), The Fundamental Research Funds for the Central Universities (No. GK202001003), Natural Science Foundation of Shaanxi Province (No. 2021JQ-313)

Corresponding author: CAO Liguo. E-mail: lgcaonju@126.com; ZHOU Zhengchao. E-mail: zczhou@snnu.edu.cn

deregg et al., 2020), floods (Bett et al., 2018; Tellman et al., 2021), and extreme precipitation events (Cao and Pan, 2014; Pan et al., 2020; Zhang and Zhou, 2020). Extreme precipitation events have attracted much research attention, and it has been studied worldwide, including Europe (da Silva et al., 2020), Asia (Li et al., 2020), South America (Bettolli et al., 2021), and Africa (Sen Roy and Rouault, 2013). For example, during the boreal summer, extreme precipitation in the Yangtze River Basin led to frequent flood disasters, which had serious ramifications (Tao and Ding, 1981; Bett et al., 2018). As the water source of the Yangtze River, the Tibetan Plateau (TP) played an irreplaceable role in extreme precipitation over this region (Wang et al., 2003; Zhao et al., 2016). Most researchers were concerned about extreme precipitation in the TP. However, only few studies have investigated the variation characteristics of light precipitation events.

Although the contribution of light precipitation to total precipitation is generally very small, light precipitation accounts for 10%–15% of the total precipitation in mid-to-high latitudes and plays an important role in the Earth system (Kidd and Joe, 2007). Light precipitation is one of the most important sources of groundwater and soil water, and decreases in its frequency increase the probability of drought (Liu et al., 2015). Jiang et al. (2014) investigated changes in precipitation intensity in different regions of China, and found that under the condition of global warming, light precipitation events have been decreasing in various regions of China. Wen et al. (2016) believed that light precipitation is closely related to heavy precipitation, and light precipitation events would decrease to some extent with increasing heavy precipitation events. Fu and Dan (2014) found that light precipitation contributed to an increase in the proportion of total precipitation and accounted for more than 60% of all precipitation days in the region covering the southeast to the northwest of China. Ueda et al. (2003) pointed out that the climatic characteristics of eastern and western TP are different. The TP has become more humid since 1990, and the wetting process is related to changes in atmospheric circulation (Sun et al., 2020). Light precipitation is believed to have significantly contributed to the wetting of the TP.

Although variations of light precipitation have received wide attention, no unified standard has been established for the definition of light precipitation. The common approach toward classifying precipitation intensity is to classify precipitation events, such as precipitation, snowfall, and hail. According to most studies, light precipitation is primarily characterized by an intensity (*Pre*) of $0.1 \leq Pre < 10.0$ mm/d (Zhai et al., 1999; Liu et al., 2005; Ma et al., 2015; Wu et al., 2017). Qian et al. (2007)and Liu et al., (2011) reported a decreasing trend of light rain events (≤ 1.0 mm/d) in China. Qian et al. (2009) defined light precipitation events as those with intensities of generally < 10.0 mm/d. In another case study, a fixed-percentile method was used to observe the characteristics of light precipitation at different stations in China (Liu et al., 2005; Wen et al., 2016). The range for light precipitation intensity was not broadly applicable to certain areas, indicating the necessity for establishing local standards to define light precipitation.

Several studies investigated the relationship between aerosol and light precipitation to determine possible causes for changes in light precipitation, and they concluded that changes in light rain could be attributed to increases in aerosol concentration (Qian et al., 2009; Qian et al., 2010; Wang et al., 2016). Aerosols indirectly affect precipitation by increasing cloud lifetime and the amount of cloud droplets. Therefore, aerosol data can be used to investigate changes in light precipitation. However, aerosol data covering different atmospheric conditions over the TP are lacking, and long-term aerosol data over the TP are difficult to obtain. Consequently, this approach is not suitable for the TP. The climate had been much warmer in the last three decades than in any decade after 1850 (IPCC, 2013), which was expected to lead to higher evaporation rates and allow the atmosphere to transport more water vapor. Therefore, the reference evapotranspiration (ET_0) is a potential factor reflecting changes in light precipitation. As water vapor affects precipitation in the TP (Feng and Zhou, 2012), it is another major factor reflecting changes in light precipitation (Zhang et al., 2013; Wu et al., 2015). Temperature changes also affect precipitation variations in China (Qian et al., 2007; Jiang et al., 2014). Climate change in China is affected by the East Asian Monsoon (Zhang et al., 2019a), which in turn is significantly affected by the Pacific Decadal Oscillation (PDO; Grigholm et al., 2009), Arctic Oscillation (AO; Zhang et al., 2017), El Niño-Southern Oscillation (ENSO; Shao et al., 2017), and North Atlantic Oscillation

(NAO; Liu and Yin, 2001). Moreover, large-scale circulation patterns (PDO, AO, ENSO and NAO) are likely to affect precipitation changes in the TP.

The TP has attracted much attention due to its particularity. The response and influence of the plateau surface environment to climate change is a hot topic of concern to scholars. However, to thoroughly understand the relevant issues, we must first conduct an in-depth study of the changes in the plateau climate in recent years. Light precipitation is an important part of precipitation in the TP area. It has an important impact on vegetation growth and soil drought on the TP. Therefore, this study investigated the variation characteristics of light precipitation in the central and eastern TP. The primary objectives of this study are 1) to analyze the temporal and spatial variability characteristics of annual light precipitation events using different precipitation intensity methods, 2) to study periodic changes in light precipitation and analyze abrupt changes, and 3) to investigate the key factors affecting the variation of light precipitation over the central and eastern TP, considering temperature, relative humidity, and large scale circulation patterns (PDO, AO, ENSO and NAO). The findings of this study are expected to enhance our understanding of light precipitation changes in the central and eastern TP and provide references for soil moisture and agricultural production in the future.

2 Materials and Methods

2.1 Study area and data description

The TP is located in the western part of China (25°N–40°N and 74°E–104°E) (Fig. 1), covering an area of approximately 3 million km^2. With an average altitude of over 4000 m, it is commonly referred to as the 'Roof of the World'. Many large rivers in South Asia, East Asia, and Southeast Asia originate from the TP. In addition, with a wide range of climatic influences and wide geographic coverage, the TP is considered the 'Third Pole' of Earth (Liu and Chen, 2000; Yao et al., 2012). There are many mountains around the TP, such as the Kunlun Mountains, Himalayas. The climate of the TP, which falls under the continental climate, is unique owing to its high altitude environment. The annual temperature range of the study area is 5–12℃, mainly affected by west and southeast winds, reflecting a typical plateau continental monsoon region (Wang et al., 2014). Precipitation primarily falls between June and September, and the total annual precipitation of the TP generally ranges from 350 to 500 mm, with higher precipitation in the southeast.

Data on daily precipitation, daily mean relative hu-

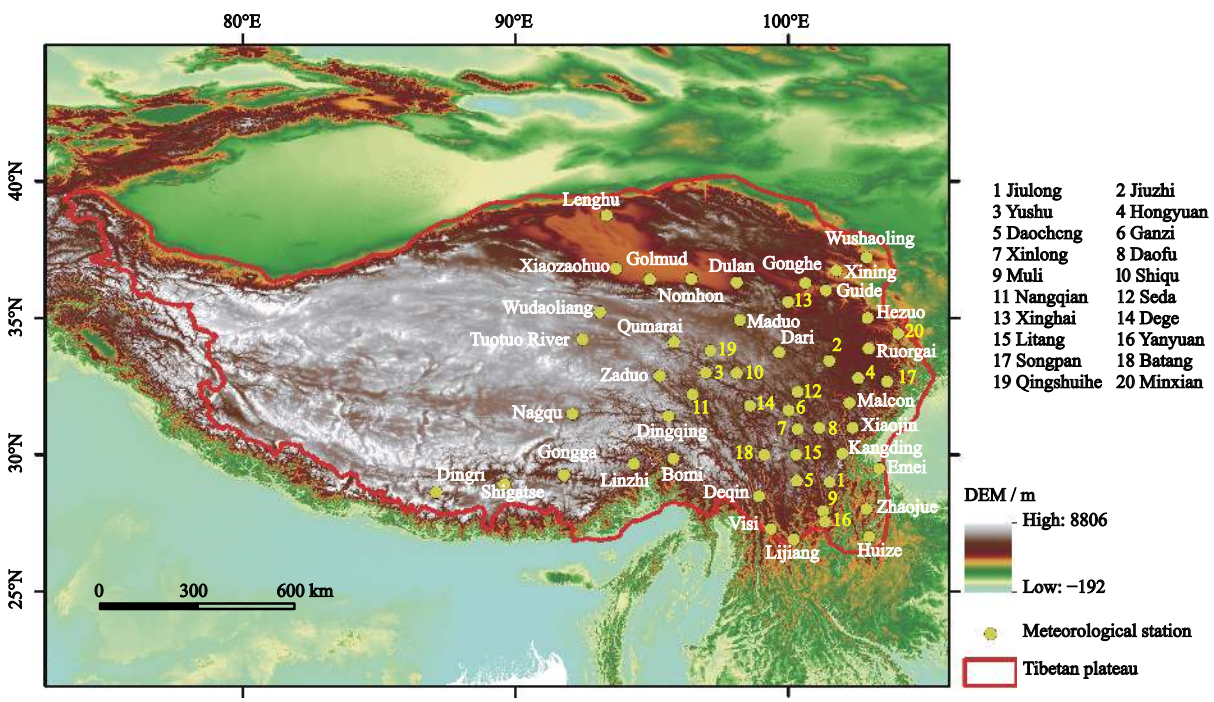

Fig. 1 Locations of meteorological stations over central and eastern Tibetan Plateau

midity, and temperature in the central and eastern of TP during 1961–2019 were obtained from meteorological stations of the National Climate Center of the China Meteorological Administration (CMA; http://data.cma.cn). We selected stations with sufficiently long-term daily data. The obtained data were subjected to strict quality control by the CMA. To ensure the representativeness of the observational data and consistency of the research time series, stations with continuous missing observations > 5 d were excluded. For station data with continuous missing observations ≤ 5 d, supplementary corrections were made through interpolation using data from adjacent stations covering the times before and after the missing dates. We finally selected data from 53 surface stations. Climatic indices (PDO, AO, ENSO and NAO) at the monthly scale were obtained from the National Environmental Information Center of the National Oceanic and Atmospheric Administration (NOAA; https://www.ncdc.noaa.gov/teleconnections/). In our analysis, we averaged the monthly values to obtain the annual mean. The ET_0 of the regional annual series was calculated as the arithmetic mean at 53 stations over the TP.

2.2 Methods

2.2.1 Definition of light precipitation events

According to the definition of CMA, a light precipitation event is generally defined as that with an intensity of < 10.0 mm/d (Qian et al., 2009). Some scholars further defined light precipitation (0.1 ≤ *Pre* < 10.0 mm/d) (Fu and Dan, 2014; Wu et al., 2017). Wu et al. (2016) used the CMA precipitation grade standards to measure daily rain rates and classified precipitation into five grades of intensity: light [0.1–10.0 mm/d); moderate [10.0–25.0 mm/d); heavy [25.0–50.0 mm/d); storm [50.0–100.0 mm/d); and downpour (≥ 100.0 mm/d). To further analyze light precipitation events, the same method can be applied to classify light precipitation into five grades of intensity: grade 1 (G1) [0.1–2.0 mm/d), G2[2.0–4.0mm/d),G3[4.0–6.0mm/d),G4[6.0–8.0mm/d), and G5 [8.0–10.0 mm/d) (Zhang et al., 2019b). We established a light precipitation assessment index (LPAI) considering the trends in such events. For one event at a given station, LPAI can be calculated as follows:

$$LPAI = G_1 \times D_1 + G_2 \times D_2 + G_3 \times D_3 + G_4 \times D_4 + G_5 \times D_5 \quad (1)$$

where G denotes the specific grade of light precipitation (1−5) and D is the number of days of light precipitation at the said grade. For example, for a light precipitation event that occurred five times a week with precipitation amounts of 1.2, 2.4, 3.9, 4.5, and 9.6 mm, its LPAI is $G_1(1) \times D_1(1) + G_2(2) \times D_2(2) + G_3(3) \times D_3(1) + G_4(4) \times D_4(0) + G_5(5) \times D_5(1) = 1 \times 1 + 2 \times 2 + 3 \times 1 + 4 \times 0 + 5 \times 1 = 13$

2.2.2 Reference evapotranspiration (ET_0)

The FAO Penman-Monteith formula is recommended by the Food and Agriculture Organization of the United Nations (FAO) for calculating ET_0 (Thornthwaite, 1951; Liang et al., 2008). A modified Penman-Monteith formula is given as follows:

$$ET_0 = \frac{0.408\Delta(R_n - G) + \gamma \frac{900}{T+273.15} U_2 (e_s - e_a)}{\Delta + \gamma(1 + 0.34U_2)} \quad (2)$$

where ET_0 is crop water requirement (mm/d); Δ is a slope at T of a temperature-saturated vapor pressure curve (kPa/℃); R_n is the daily net radiation at the surface [MJ/(m^2·d)]; G is soil heat flux (MJ/(m^2·d)); γ is the psychrometric constant (kPa/℃); T is the average air temperature at 2 m (m/s); U_2 is the daily wind speed at 2 m height (m/s); e_s is the saturation vapor pressure (kPa); e_a is actual vapor pressure (kPa).

2.2.3 Mann-Kendall (M-K) test and abrupt change analysis

The Mann Kendall statistical test is a non-parametric test widely used in hydro-meteorological data analyses (Silva et al, 2015). The null hypothesis H_0 states that deseasonalized data $(x_1,..., x_n)$ are a sample of n independent events, and x_i is independent and identically distributed. The alternative hypothesis H_1 states that a monotonic trend exists in X. The Kendall statistic S is estimated as follows:

$$S = \sum_{i=1}^{n-1} \sum_{j=i+1}^{n} \operatorname{sgn}(x_j - x_i) \quad (3)$$

where x_j is the value of sequential data, n is the length of the data set, and

$$\operatorname{sgn}(\theta) = \begin{cases} +1 & for\ \theta > 0 \\ 0 & for\ \theta = 0 \\ -1 & for\ \theta < 0 \end{cases} \quad (4)$$

When $n \geq 8$, the statistic S is approximately normally distributed with the mean and the variance as follows (Mann, 1945; Kendall, 1981).

$$E(S) = 0$$
$$Var(S) = \frac{n(n-1)(2n+5) - \sum_{m}^{n} t_m(m)(m-1)(2m+5)}{18} \quad (5)$$

where n is the length of the data set, t_m denotes the number of ties of extent m. The test statistic Z_c is computed as follows:

$$Z_c = \begin{cases} \dfrac{S-1}{\sqrt{Var(S)}}, & S > 0 \\ 0, \quad S = 0 \\ \dfrac{S+1}{\sqrt{Var(S)}}, & S < 0 \end{cases} \tag{6}$$

where Z_c is the test statistics. If $|Z_c|$ is greater than $Z_{1-\alpha/2}$, in which the standard normal deviates and α is the significance level for the test, then the trend is significant.

2.2.4 Period analysis

The Morlet wavelet is an exponential complex-valued wavelet adjusted by a Gaussian window; it has the characteristics of non-orthogonality and can provide information on the amplitude and phase of a time series (Tian et al., 2014). Therefore, Morlet wavelet analysis is widely used in climate and meteorological cycle analysis (Cao et al., 2014; Cao and Pan, 2014; Wang et al., 2014). The function of the Morlet wavelet is as follows:

$$\varphi(K\omega) = \frac{\pi^{-\frac{1}{4}} H(\omega) e^{-(K\omega-\omega_0)^2}}{2} \tag{7}$$

where K is the wavelet scale; ω is frequency; $H(\omega)$ = Heaviside step function, $H(\omega) = 1$, if $\omega > 0$, $H(\omega) = 0$ otherwise; ω_0 is the nondimensional frequency.

3 Results

3.1 Characteristics of annual precipitation

Fig. 2a shows the average annual precipitation of the central and eastern TP. From 1961 to 2019, average annual precipitation exhibited an obvious upward trend on the whole. The increase in precipitation mainly started in 1980 with yearly fluctuations; before 1980, precipitation was below average (511.3 mm) in most years. There was a significant increase in precipitation from 1979 to 1980 and 1997 to 1998, and the average annual precipitation in 1998 was significantly higher than that in other years, reaching 651.7 mm (Fig. 2a). The lowest average annual precipitation occurred in 1972, with a precipitation of only 443.9 mm. The average annual precipitation was 537.5 mm, which was lower than the median annual precipitation (541.5 mm). Annual precipitation was outside the range of the 25th–75th percentiles in most years, indicating high risk of flood and drought in the central and eastern TP. Fig. 2b shows that precipitation was mainly concentrated in summer from June through September, accounting for approximately 77.9% of the average annual precipitation. Moreover, precipitation from June to August exceeded 80.0 mm. This result is similar to the conclusion of Xu et al. (2008), who reported that most of the precipitation in central and eastern TP occurred from June through September, accounting for more than 60%–90% of the annual total.

From the spatial distribution of the average annual precipitation in the central and eastern TP from 1961 to 2019 (Fig. 3a), precipitation presented an increasing trend from the northwest to the southeast, which can be explained by the wet stream from the Bay of Bengal being blocked by the Himalayas and redirected northwest along this range, creating an east-west precipitation gradient (Maussion et al., 2014). Thus, the maximum precipitation occurred in the Three River Headwaters Region in the southeast of the central and eastern TP, even exceeding 165.0 mm. The Dingqing, Bomi, and Nyingchi stations in Tibet and the Kangding, Songpan, and Emeishan stations in Sichuan are located at two

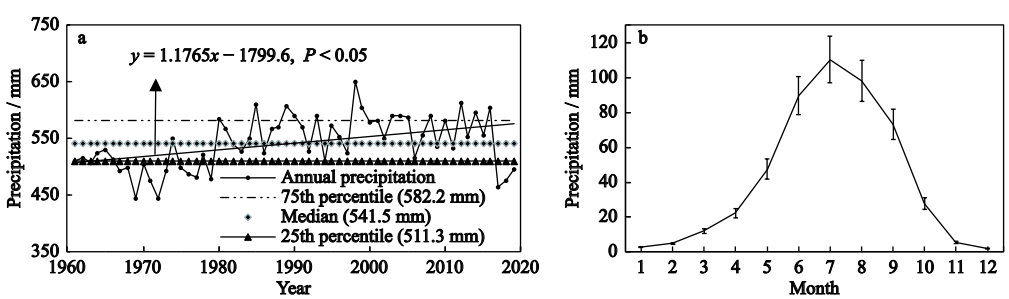

Fig. 2 The average annual and monthly precipitation over the central and eastern Tibetan Plateau from 1961 to 2019. a: annual series of total precipitation; b: monthly changes of precipitation, error bars represent one standard deviation of inter-annual variation of precipitation in each month

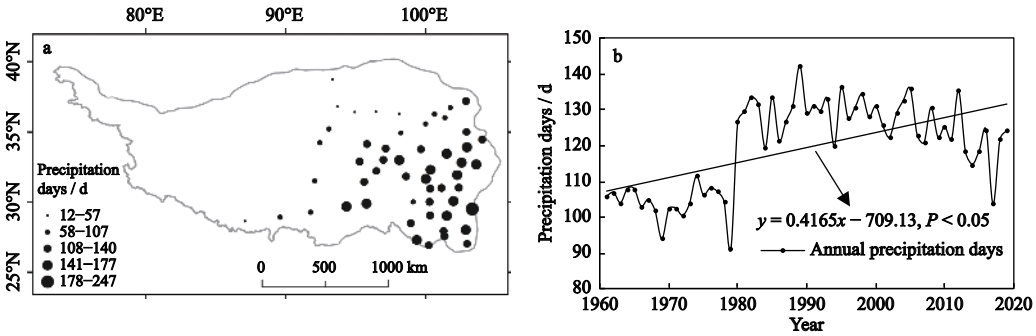

Fig. 3 Spatial distribution of precipitation days (a) and annual precipitation days averaged (b) over the central and eastern Tibetan Plateau from 1961 to 2019

heavy precipitation centers in the southeast of the central and eastern TP. In all these areas, precipitation exceeded 145.0 mm. The least precipitation (< 50.0 mm) was observed in the Qaidam Basin in the northern part of the study area, which is the driest region. The number of precipitation days showed a significant increasing trend of 4.2 d/10 yr over the central and eastern TP (Fig. 3b), and this result is consistent with that of Ge et al. (2008). The average annual precipitation days were 124 d at all meteorological stations in the central and eastern TP (Fig. 3b).

3.2 Temporal and spatial characteristics of annual light precipitation

Fig. 4 shows the spatial and temporal variation characteristics of light precipitation during the 59 yr in the central and eastern TP. As shown in Fig. 4a and b, the spatial variations of the amount and number of days of light precipitation were consistent, and they gradually increased from the northwest to the southeast. The minimum value of light precipitation was observed in the northwestern part of the central and eastern TP, which was represented by Lenghu (14.0 mm) and Xiaozaohuo (25.0 mm) in the Qaidam Basin. The maximum of total amount of light precipitation (288.6 mm) was observed in the southeastern part of the plateau, represented by Bomi in Tibet, Songpan in Sichuan (272.3 mm), and Hongyuan in Sichuan (258.5 mm) (Fig. 4a). The number of light precipitation days in the southeast region was more than 90 days while the northwest of the central and eastern TP showed lower values (< 60 d) (Fig. 4b). The characteristics of spatiotemporal changes of light precipitation are very similar to spatiotemporal changes of precipitation. As shown in Fig. 4c and d, the proportion of light precipitation days in the total precipitation days showed the same spatial variation trend as the proportion of light precipitation in the total precipitation amount. The amounts and days of light precipitation and the spatial distribution of the proportion of light precipitation appeared to completely oppose each other (Figs. 4 a–d). The northern and northwestern parts of the central and eastern TP exhibited low values of light precipitation and days, but they accounted for a high percentage of precipitation. This is in line with the abovementioned reasons for the differences in the spatial distribution of precipitation over the central and eastern TP. In addition to the northwestern part of the central and eastern TP experiencing less precipitation, light precipitation accounted for a larger proportion of the total precipitation. The annual average light precipitation days were 71 d and light precipitation was 165.0 mm (Fig. 4e). In the 59 yr period, the overall light precipitation days in the central and eastern TP appeared to be slowly increasing at a rate of approximately 2–4 d/10 yr. The amounts of light precipitation exhibited the same trend as the number of days of precipitation, with an overall increase rate of approximately 4.0–6.0 mm/10 yr. Among the 53 meteorological stations in the central and eastern TP, only 12 stations, mainly in Sichuan and Yunnan provinces in the eastern part of the central and eastern TP, showed a downward trend, accounting for 22.6% ($Pre < 0.05$). The amounts of light precipitation and the number of light precipitation days accounted for 30.7% and 81.5%, respectively, of the corresponding total values (Fig. 4f). Similarly, the statistics for 1951–2002 showed that over the eastern edge of the central and eastern TP, precipitation mainly occurred in the form of light-moderate precipitation in terms of both the amounts and number of days, accounting for 66.9% and 96.9%, respectively (Li et al., 2010). As shown in

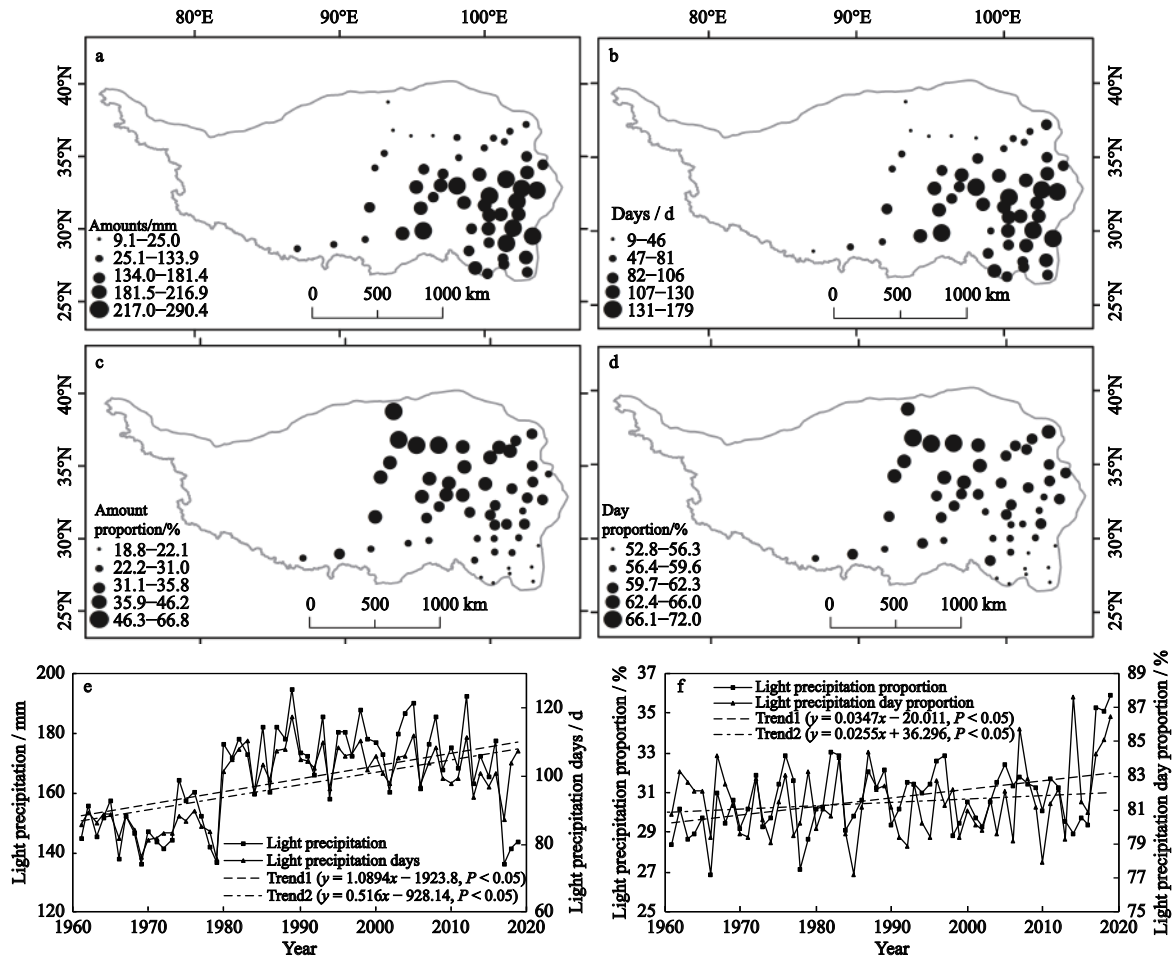

Fig. 4 Spatial and temporal characteristics of light precipitation events. a: light precipitation amounts; b: light precipitation days; c: light precipitation amount proportion in total precipitation; d: light precipitation day proportion in total precipitation; e: annual changes of light precipitation amounts and days; and f: annual proportions in total precipitation amounts and days

Figs. 4e and f, we found that light precipitation changed dramatically around 1980 and 1998. During the El Niño event from 1997 to 1998, strong westerly anomalies occurred on the southern side of the central and eastern TP, inducing precipitation or snow over large areas of the central and eastern TP and south of the Yangtze River (Tao et al., 1998). Light precipitation increased in both the number of rainy days and intensity in 1998, but the proportion of light precipitation exhibited a downward trend, indicating that the increase of heavy precipitation during the 1997–1998 period exceeded that of light precipitation. Changes in precipitation would be affected by various factors, especially in the sensitive area of the central and eastern TP. The abrupt influence of light precipitation in 1980 was more complicated and needs to be investigated further in the future.

For a more in-depth analysis of the spatial and temporal changes of light precipitation, we classified light precipitation into five grades of intensity (G1–G5). Fig. 5 presents the temporal and spatial characteristics of G1 light precipitation events over the TP from 1961 to 2019. As presented in Fig. 5a, the amounts of G1 light precipitation have the same spatial variation trend as that shown in Fig. 4a. The minimum amount of G1 light precipitation (< 23.0 mm) was observed in northern TP with an increasing gradient to southeast TP (> 30.0 mm). Among the 53 meteorological stations in the central and eastern TP, only 15 stations presented a downward trend, accounting for 28.3% (P < 0.05), mainly in Sichuan and Yunnan provinces in the south and southeast TP (Fig. 5a). Areas with low values of G1 light precipitation corresponded to those with low values of the total amount of light precipitation, and they were located in the Lenghu and Qaidam Basin. This further confirmed that the northwestern part of the central and eastern TP mainly experienced light precipitation. The spa-

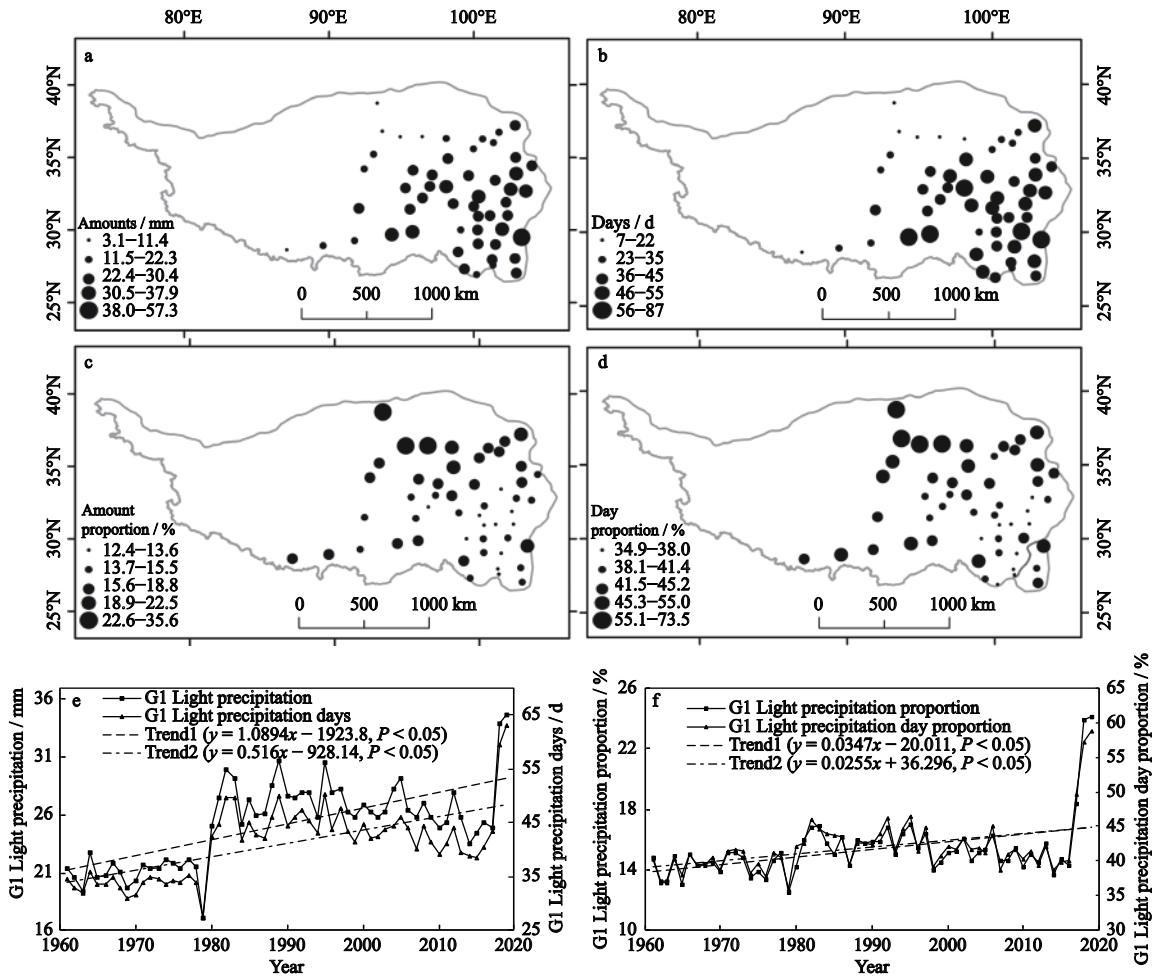

Fig. 5 Spatial and temporal characteristics of G1 light precipitation events. a: G1 light precipitation amounts; b: G1 light precipitation days; c: G1 proportion in total light precipitation amount; d: G1 day proportion in total light precipitation days; e: annual changes of G1 light precipitation amounts and days; f: annual proportions in total light precipitation amounts and days

tial variation trends of the days and amounts of G1 light precipitation appeared to be the same (Fig. 5b). In most areas, the proportion of the amount of G1 light precipitation was 12%–20% (Fig. 5c), while days of G1 light precipitation accounted for more than 35% of the total light precipitation (Fig. 5d). As presented in Figs. 5a–d, the spatial distribution of G1 light precipitation was opposite to the proportion of its amounts and days. From the perspective of precipitation, G1 light precipitation did not significantly affect the entire area, but from the perspective of precipitation days, it had a pivotal effect. Fig. 5e shows the annual average days (25 d) and amounts (41.0 mm) of G1 light precipitation. As shown in Fig. 5f, the proportions of the annual average days and amounts of G1 light precipitation were 42.0% and 15.3%, respectively. The amounts and days of G1 light precipitation were consistent with the annual change trend of the proportion of G1 light precipitation to total light precipitation. An overall increasing trend was observed before 1983 and a decreasing trend was observed after 1983. In addition, significant upward changes were observed around 1980. From the above-mentioned results, G1 light precipitation accounted for more than 30.0% of the total light precipitation events in the study region. During the 59 yr, most meteorological stations with G1 light precipitation recorded upward trends for days and amounts. The above results indicated that G1 light precipitation events accounted for a much larger proportion of the total light precipitation events than other intensities of light precipitation. Therefore, G1 light precipitation over the central and eastern TP would be worth paying attention.

The amounts of G2 and G3 light precipitation showed the same obvious spatial variation characteristics

(Figs. 6a and 7a), with higher values in the southeast (> 39.0 mm) and lower values in the northwest (< 28.0 mm). Most of the stations with G2 and G3 light precipitation days and amounts recorded an increasing trend and accounted for more than 70% of all stations. Most of these stations were distributed in the southeast TP (Figs. 6a and 7a). The days and amounts of G2 and G3 light precipitation exhibited the same spatial variation trend (Figs. 6b and 7b). The proportions of the amounts and days of G2 light precipitation exhibited the same spatial variation trends (Figs. 6c and d). However, these trends were diametrically opposite to those of G2 light precipitation. The proportions of the days and amounts of G2 light precipitation were gradually decreasing from the north and center to the southeast, while the amount of G2 light precipitation was increasing from the north to the southeast. G2 and G3 light precipitation events ($2.0 \le Pre < 6.0$ mm/d) not only exhibited the same spatial variation but also exceeded G1 light precipitation ($0.1 \le Pre < 2.0$ mm/d). However, the frequency of G1 light precipitation was significantly higher in the number of precipitation days. Fig. 6e shows that the annual average days and amounts of G2 light precipitation were 12 d and 33.5 mm, respectively. As shown in Fig. 6f, the proportions of the annual average days and amounts of G2 light precipitation were 12.5% and 22.3%, respectively. As shown in Fig. 7e, the annual average days and amounts of G3 light precipitation were 8 d and 36.8 mm, respectively. As presented in Fig. 5f, the proportions of the annual average days and amounts of G1 light precipitation were 7.8% and 22.3%, respectively. Before 1980, the proportions of the amounts and days of G2 light precipitation showed the same trend. Between 2016 and 2019, the proportion of

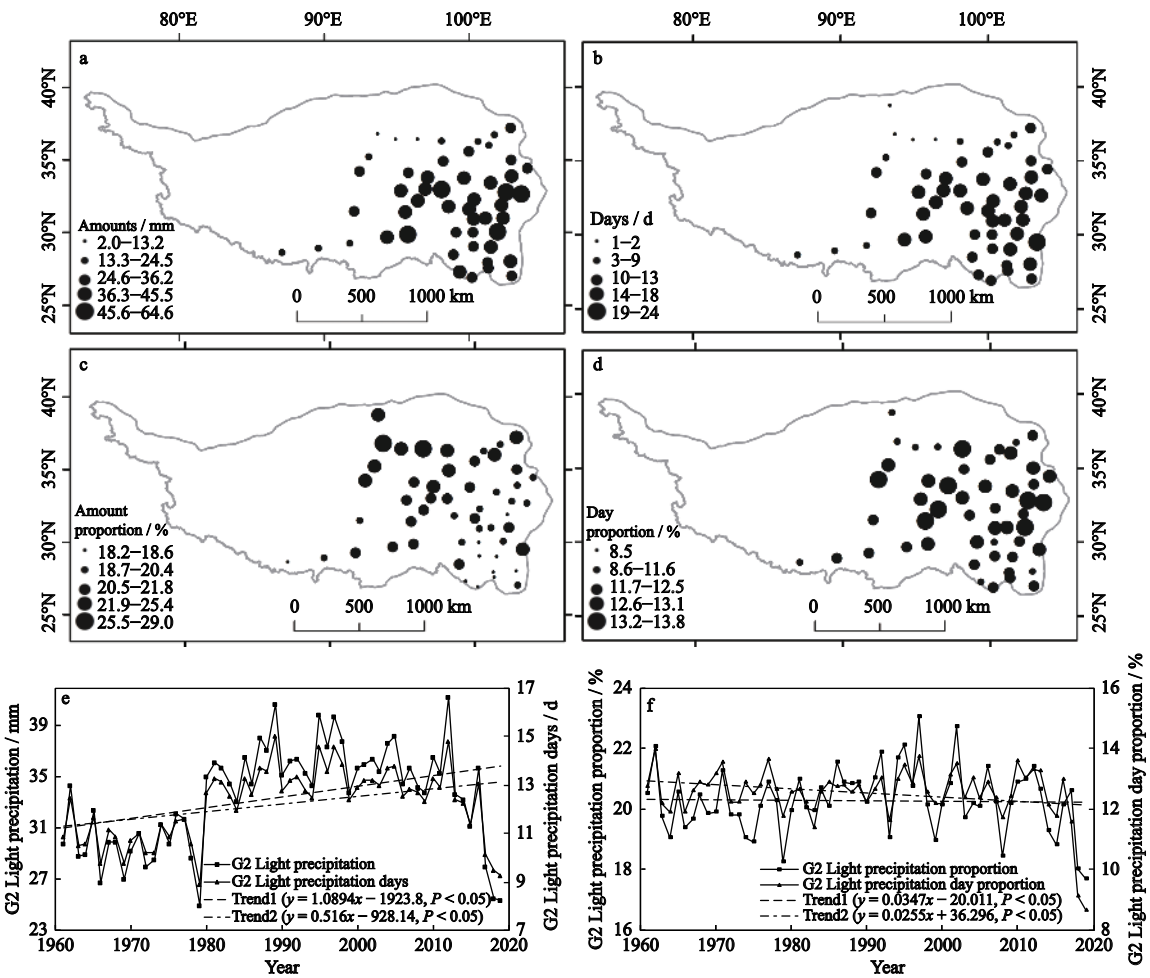

Fig. 6 Spatial and temporal characteristics of G2 light precipitation events. a: G2 light precipitation amounts; b: G2 light precipitation days; c: G2 proportion in total light precipitation amount; d: G2 day proportion in total light precipitation days; e: annual changes of G2 light precipitation amounts and days; f: annual proportions in total light precipitation amounts and days

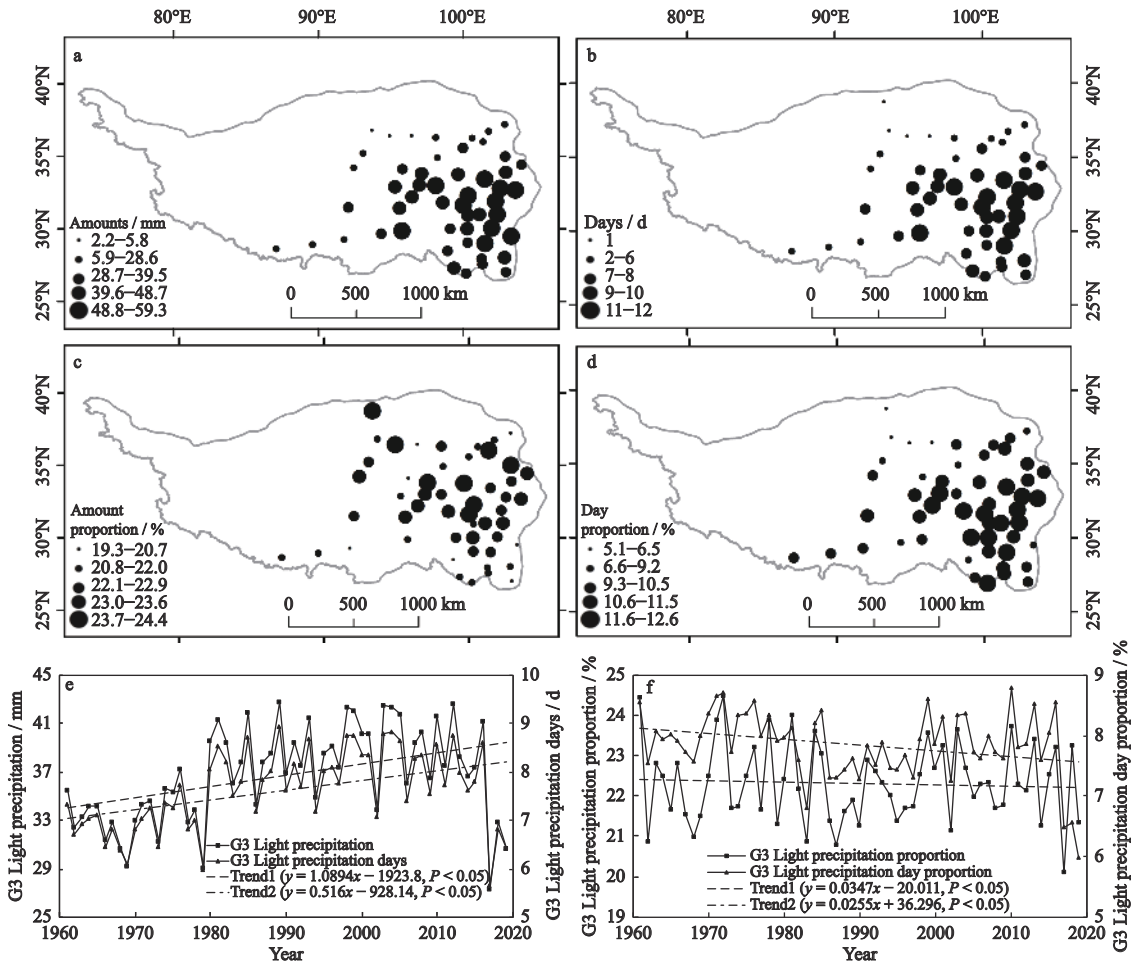

Fig. 7 Spatial and temporal characteristics of G3 light precipitation events. a: G3 light precipitation amounts; b: G3 light precipitation days; c: G3 proportion in total light precipitation amount; d: G3 day proportion in total light precipitation days; e: annual changes of G3 light precipitation amounts and days; f: annual proportions in total light precipitation amounts and days

the days of G2 light precipitation decreased and that of the amounts increased. These changes can probably be attributed to increases in the amounts and days of G1 light precipitation. Similarly, the proportions of the amounts and days of G3 light precipitation declined from 2016 to 2019.

As most of the observing stations are located in the southeast of the central and eastern TP, approximately 81.1% of the observing stations showed a slight upward trend for G4, with obvious spatial variation characteristics (Fig. 8a). Higher (> 35.0 mm) and lower (< 24.0 mm) amounts of amounts of G4 light precipitation were observed in the southeast and north. The spatial variation trend of the annual average days of G4 light precipitation was the same as that of the amounts, increasing from < 3 d in the northwest to > 5 d in the southeast (Fig. 8b). The proportions of the amounts and days of G4 light precipitation exhibited similar spatial variation trends (Figs. 8c and d). Fig. 8e shows the annual means of the amounts (32.4 mm) and days (5 d) of G4 light precipitation. As shown in Fig. 8f, the proportions of the annual mean days and amounts of G4 light precipitation were 4.8% and 19.6%, respectively.

As presented in Fig. 9a, the spatial trend of G5 light precipitation was basically the same as that of G4 (Figs. 9a and b). The lowest G5 light precipitation (< 28.2 mm) was observed in the north and increased to the southeast (> 41.8 mm) of the area. This can be attributed to most of these stations being located in the southeast of central and eastern TP, and the upward trend was recorded in approximately 69.8% of the stations (Fig. 9a). The proportions of the amounts and days of G5 light precipitation were similar to those of G4 (Figs. 9c and d). Fig. 9e shows the annual average days (4 d) and amounts (37.0 mm) of G5 light precipitation. As shown in Fig. 9f, the proportions of the annual mean

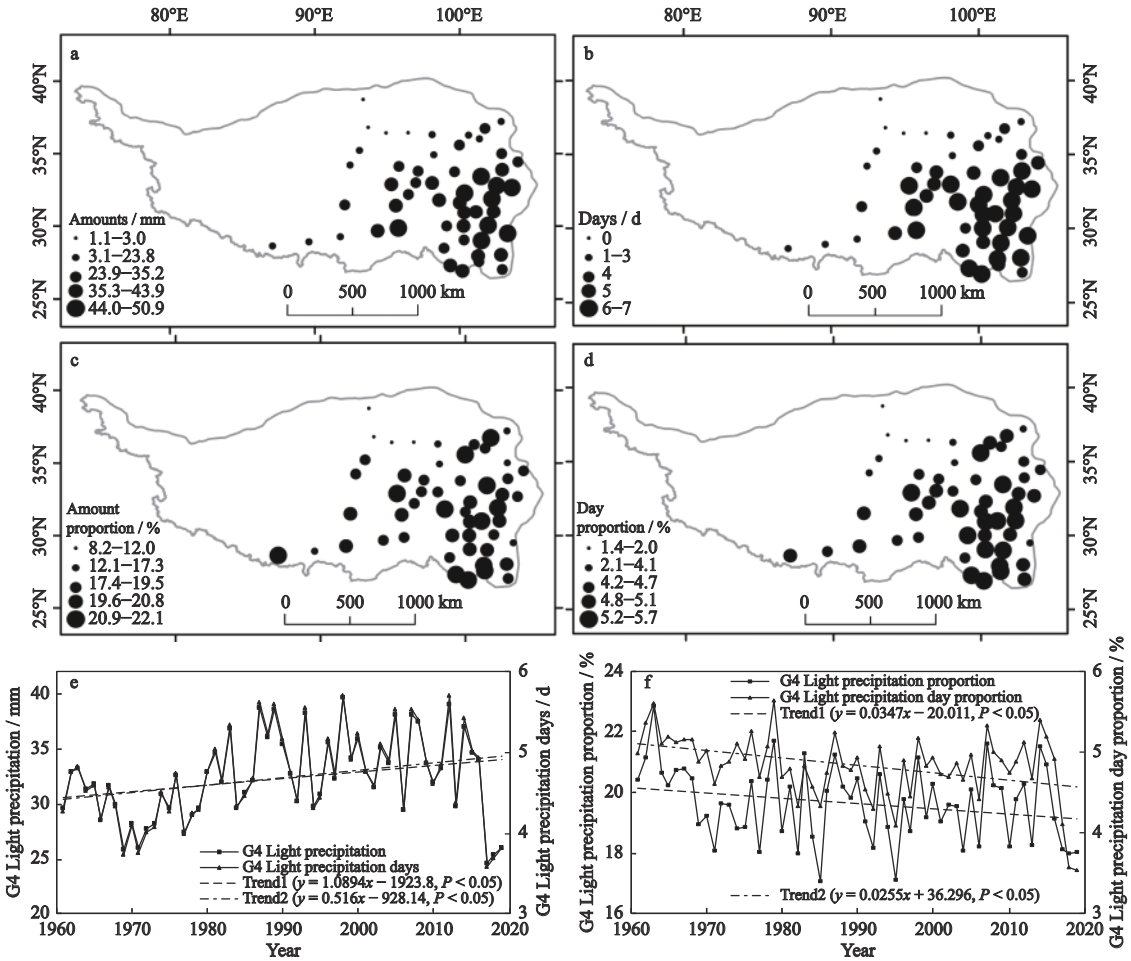

Fig. 8 Spatial and temporal characteristics of G4 light precipitation events. a: G4 light precipitation amounts; b: G4 light precipitation days; c: G4 proportion in total light precipitation amount; d: G4 day proportion in total light precipitation days; e: annual changes of G4 light precipitation amounts and days; f: annual proportions in total light precipitation amounts and days

days (4.3%) and amounts (22.4%) of G5 light precipitation declined.

To comprehensively investigate the spatial distribution of different intensities of light rain over the entire region, we divided light precipitation into 5 levels and calculated the light precipitation assessment index (LPAI) for the entire study area (Fig. 10). LPAI showed high performance in the east and west and low performance in the middle. Through the spatial distribution of LPAI, we can more accurately ascertain that light precipitation occurs more frequently in the southeast of the TP. According to the analysis of G1–G5 light precipitation, we could conclude that G1 light precipitation accounted for the least amount (41.0 mm) but the most days (25 d). The amounts of G2, G3, G4, and G5 light precipitation were similar (ca. 30.0 mm), but the number of days decreased from G1 to G5. The number of G1 days accounted for 35% of the total light precipitation days; increasing light precipitation trends can be attributed to changes in G1 events ($0.1 \leq Pre < 2.0$ mm/d). This is because the increasing trends of the days and amounts of G1 light precipitation are more prominent than those of the others. Therefore, the spatial distribution of G1 light precipitation affects the spatial variation of LPAI.

3.3 Abrupt change analysis

We applied the Mann-Kendall (M-K) method at the 0.05 significance level for G1–G5 light precipitation and LPAI. The analysis results are summarized in Table 1. All the factors exhibited abrupt changes to some extent, and these abrupt changes are worth exploring. As shown in Fig. 4e, the amounts and days of light precipitation in TP exhibited an increasing tendency from 1961 to 2019, with an abrupt change in 1980. Fig. 2a and Fig. 3b also show the same abrupt change in the amounts and days

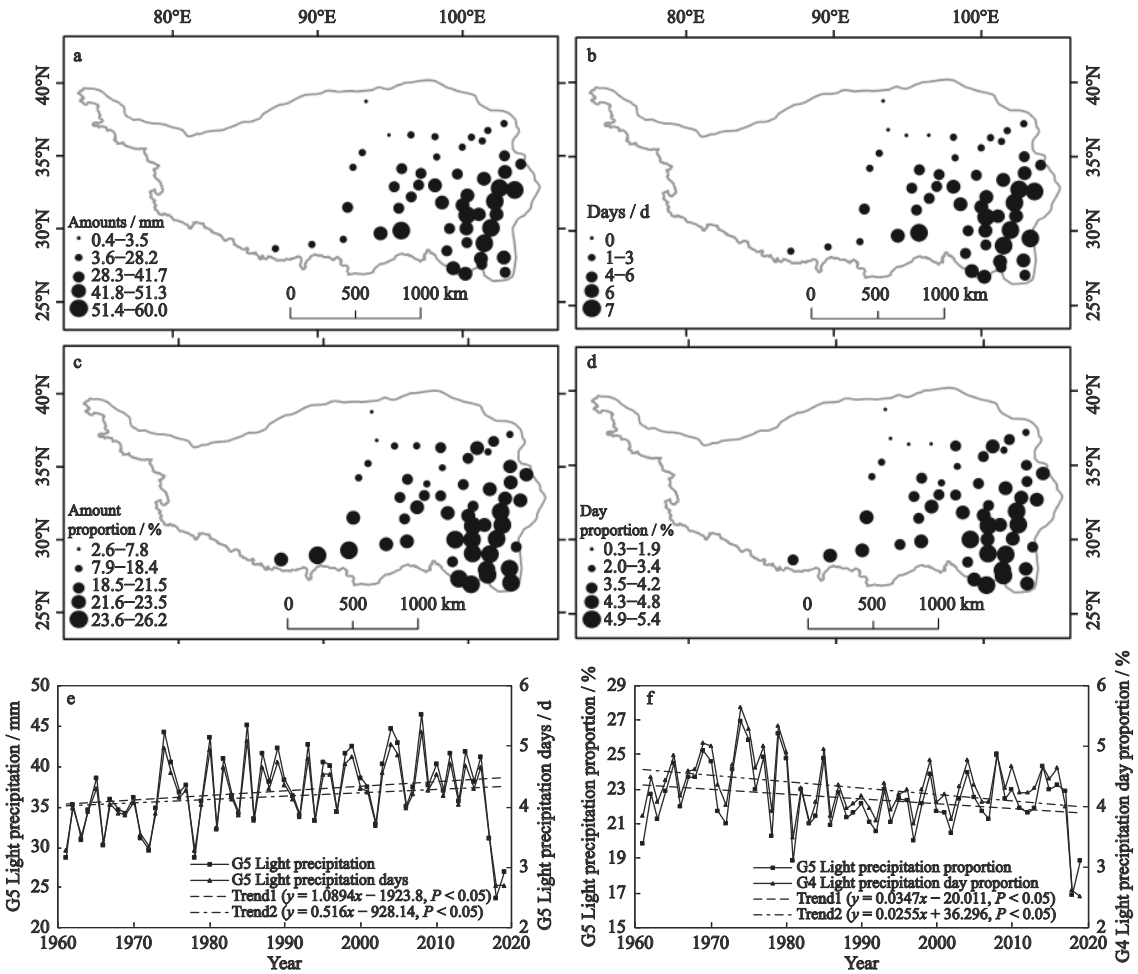

Fig. 9 Spatial and temporal characteristics of G5 light precipitation events. a: G5 light precipitation amounts; b: G5 light precipitation days; c: G5 proportion in total light precipitation amount; d: G5 day proportion in total light precipitation days; e: annual changes of G5 light precipitation amounts and days; f: annual proportions in total light precipitation amounts and days

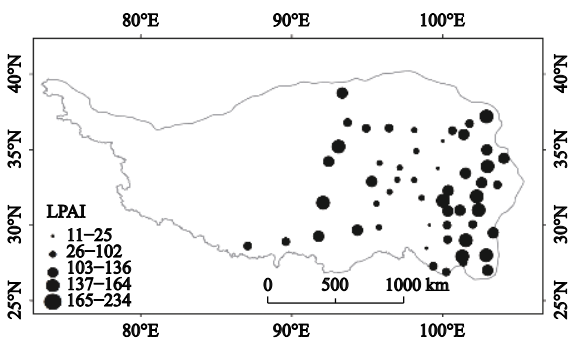

Fig. 10 Spatial characteristics of the light precipitation assessment index (LPAI) over the central and eastern Tibetan Plateau

Table 1 Trend and abrupt change of G1–G5 light precipitation and light precipitation assessment index (LPAI)

Grade	M-K trend Confidence/%	Abrupt change year
G1	95	1974
G2	95	1979
G3	95	1980
G4	95	1983
G5	95	1979
LPAI	95	1979

of precipitation in 1980, after which precipitation prominently increased in the TP. In Fig. 5e, a sudden change in G1 light precipitation appeared in 1980, but the M-K test showed that the sudden change in G1 light precipitation appeared in 1974. As the exact beginning time of the abrupt change cannot be determined from Fig. 5e, the year of abrupt change can be ascertained to be around 1980. In the middle of the 1970s, the east of the TP experienced a climatic jump, with abrupt changes in snow-accumulation days, regional average annual precipitation, and surface pressure (Niu et al., 2004). This abrupt climate change might have significantly affected

G1 light precipitation. Combining the results of the M-K test and the results shown in Fig. 6e, Fig. 9e, and Fig. 10, the year of the abrupt changes in G2 and G5 light precipitation and LPAI can be ascertained to be 1979. Accordingly, abrupt changes in G3 and G4 light precipitation occurred in the years of 1980 and 1983, respectively.

3.4 Relationship between LPAI and large-scale atmospheric circulation

In order to further characterize the causes of changes in light precipitation, correlation analysis was conducted to study the relationship of G1–G5 light precipitation and LPAI with four climate indices (ENSO, NAO, AO and PDO), ET_0, temperature (TEM), and relative humidity (RHU) (Fig. 11). In general, the correlation of G1–G5 light precipitation and LPAI with temperature was statistically significant at the 0.05 level, indicating stronger influence of temperature on G1–G5 light precipitation and LPAI compared to other indicators. Fig. 11 shows a positive correlation of temperature with G1–G5 light precipitation and LPAI, implying that the rising temperature was conducive to the formation of light precipitation events in the TP. Although the correlation of G1–G5 light precipitation and LPAI with the four climate indices, ET_0, and RHU was not statistically significant, the effects of these factors on changes in light precipitation still need to be considered. Our analysis revealed that G1 light precipitation had the highest correlation with the four climate indices and they were positively correlated, among which the correlation with PDO reached 0.42. It can thus be concluded that G1 light precipitation was more sensitive to these four climate indices. We also found that the RHU had a small impact on light precipitation, with a correlation below 0.3 ($P < 0.05$). Many scholars found that water vapor has a significant correlation with light precipitation in other regions (Liu et al., 2011; Wu et al., 2015). The correlation between RHU and light precipitation in the central and eastern TP was not significant, and the reasons might be more complicated. Therefore, the relationship between light precipitation and water vapor in the central and eastern TP area requires further investigation in order to determine the complex factors affecting changes in light precipitation. Studies have reported that the aerosol concentration of the TP had been continuously changing in the past few decades (Lau et al., 2006; Huang et al., 2007; Cong et al., 2007). Many researchers believe that changes in aerosol concentration in the atmosphere might affect changes in light precipitation (Qian et al., 2009; Zhao et al., 2006). Aerosols might increase the number of droplets while reducing droplet size, thereby inhibiting light precipitation (Gong et al., 2007). However, long-term aerosol data over the central and eastern TP are lacking. The accuracy of the correlation is difficult to verify using the results of short-term aerosol data.

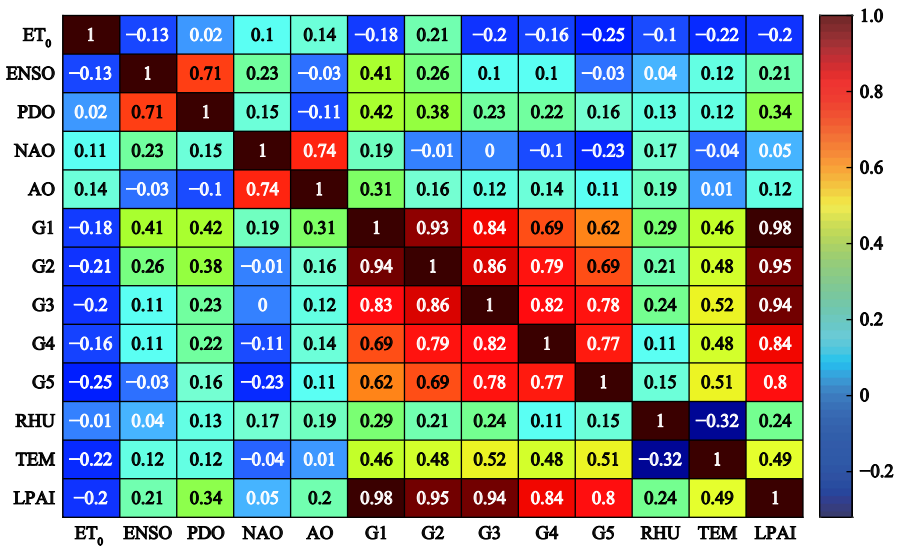

Fig. 11 Correlation coefficients between the light precipitation assessment (LPAI) and large-scale atmospheric circulation over the central and eastern Tibetan Plateau. ET_0, the reference evapotranspiration; ENSO, El Niño-Southern Oscillation; PDO, Pacific Decadal Oscillation; NAO, North Atlantic Oscillation; AO, Arctic Oscillation; G1–G5, grade of light precipitation events; RHU, relative humidity; TEM, temperature

3.5 Period analysis

Fig. 12 presents the time-frequency distributions of G1–G5 light precipitation and LPAI over the TP during 1961–2019 in the real part of the Morlet wavelet. Fig. 12a shows that G1 light precipitation had 7 yr and 8 yr cycles, with significant oscillations. As presented in

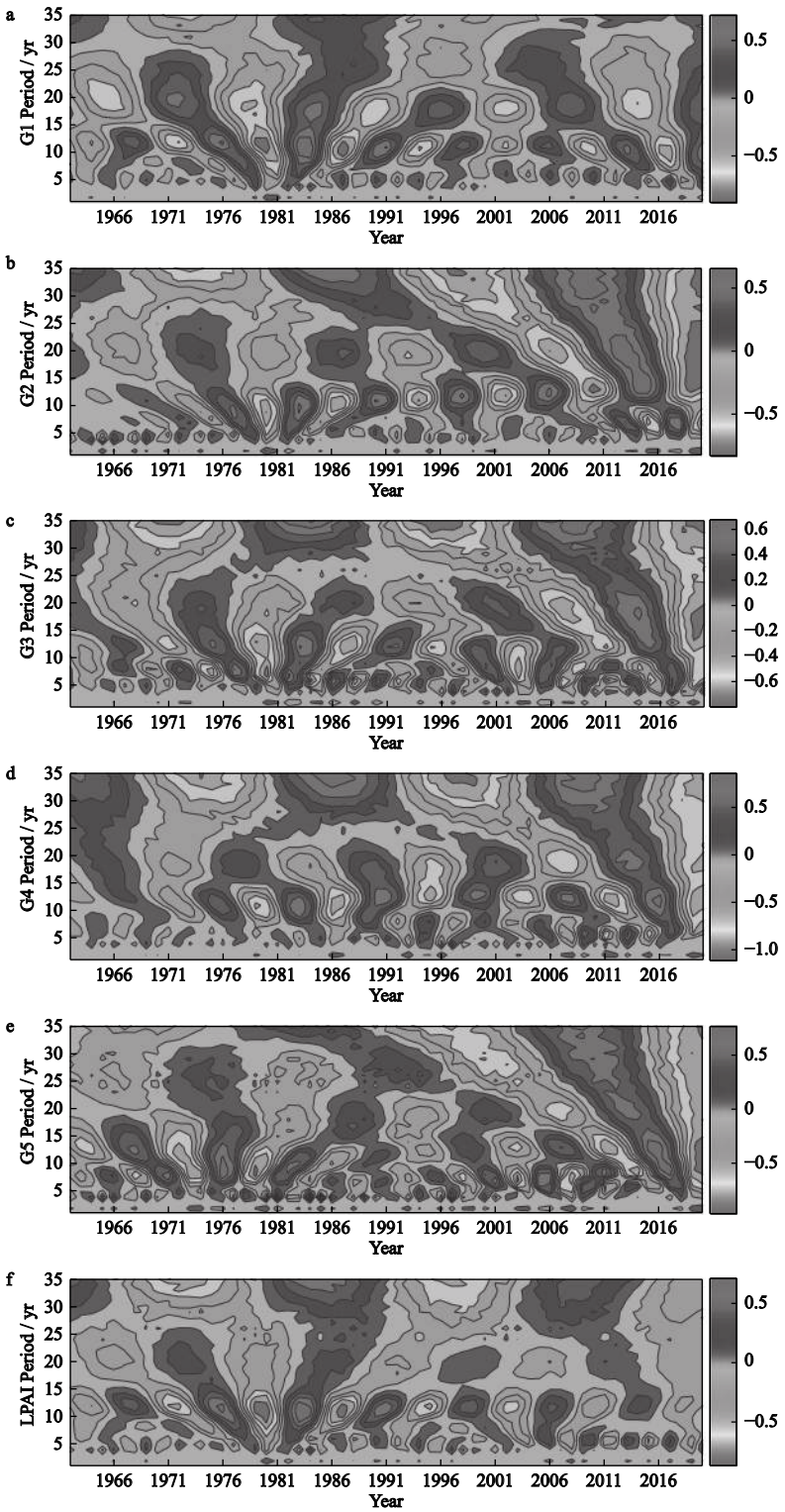

Fig. 12 The real part of the Morlet wavelet analysis of the G1–G5 light precipitation and light precipitation assessment index (LPAI) over the central and eastern Tibetan Plateau from 1961 to 2019

Fig. 12b, G2 light precipitation had 5 yr and 9 yr cycles. The 9 yr cycle, which mainly occurred from 1972 to 1981, was the most significant cycle in the entire time series. As shown in Fig. 12c, G3 light precipitation had 2 yr and 5 yr cycles, and the main cycle was 5 yr. Fig. 12d shows that G4 light precipitation had 6 yr and 7 yr cycles. In the entire time series, the 6 yr cycle was the most noteworthy. As shown in Fig. 12e, G5 light precipitation had 2 yr, 4 yr, and 6 yr cycles, and the main cycle was 6 yr. The LPAI had 6 yr and 13 yr cycles (Fig. 12f), and the dominant cycle was 6 yr.

4 Discussion

In this study, We observed that the annual precipitation amount did not exhibit any obvious growth trend over the central and eastern TP (approximately 1.1 mm per year). Zhang et al. (2015) also reported similar results that the annual precipitation increased by about one millimeter per year over the last 52 yr in the TP. However, the number of precipitation days exhibited a trend of significant increase. The number of light precipitation days accounted for 81.5% of the total precipitation days in the central and eastern TP. Accordingly, we infer the increase in precipitation day count to be mainly attributable to the significant increase in the number of light precipitation days. Li et al. (2010) also believed that the number of rainy days and the amount of total precipitation have changed from the 1950s to the 1970s in association with light-moderate precipitation over the eastern edge of the central and eastern TP. In summary, the amount and days of precipitation over the central and eastern TP were mainly affected by changes in light precipitation.

We also analyzed the spatial distribution of precipitation in the central and eastern TP. In the central and eastern TP, precipitation is mainly concentrated in the southeast, and showed a decreasing trend from the southeast to the northwest. We observed that the temporal and spatial variation trend of light precipitation had the same spatial distribution as that of central and eastern TP. This coincided with the abovementioned conclusion that light precipitation is the main factor affecting precipitation in the central and eastern TP. This spatial distribution can be mainly attributed to the towering Himalayas running east to west and the Naga Mountains in western Myanmar running north to south, which form a horseshoe–shaped terrain with the opening in the southwest. When warm southerly winds blow from the Bay of Bengal into the horseshoe–shaped terrain in summer, the airflow is forced into a cyclonic bend. The frequencies of the northeast and southwest winds are not significantly different, and a monsoon convergence zone is consequently formed, which increases precipitation in the area (Wu and Zhang, 1998; Duan et al., 2013). The low precipitation in the northwestern TP and the Qaidam Basin could be attributed to the deep interior of the Qaidam Basin. Plateaus and mountains on the side may also block the southeast monsoon from the effects of the Pacific Ocean. The Kunlun Mountains on the south and the Qilian Mountains on the north hinder the weak Atlantic and Arctic water vapor from entering the basin, and the lack of external water vapor transportation leads to a decrease in precipitation in the basin. Therefore, a phenomenon of precipitation increasing from the northwest to the southeast occurs in the TP.

According to previous studies, we set the range of light precipitation at $0.1 \leq Pre < 10.0$ mm/d (Qian et al., 2009; Fu and Dan, 2014; Wu et al., 2017). Through our calculations, we found a significant increase in the amounts and days of annual light precipitation in the central and eastern TP. However, this threshold did not accurately reflect the trend of light precipitation. To determine a threshold more suitable for the central and eastern TP, we divided it into five grades (G1–G5). Although G1 precipitation accounted for only approximately 14% of the total amount of precipitation, the number of days of G1 precipitation accounted for more than 40%. Therefore, we believe that G1 ($0.1 \leq Pre < 2.0$ mm/d) is more in line with the light precipitation standard over the central and eastern TP. This conclusion also agrees with the threshold of light precipitation in China reported by Liu et al. (2011).

We performed the M-K test and Morlet wavelet analysis to investigate the long-term series of precipitation variation data. We observed that the abrupt changes in precipitation were mainly concentrated in 1980. Some scholars also found that changes in many meteorological factors, including RHU, total cloud amount, regional average temperature, sunshine duration, and surface pressure, in certain areas corresponded to the same change in 1980 (Niu et al., 2004; You et al., 2010). Previous studies found that solar irradiance, total cloud

cover, and air temperature are strongly correlated with changes in light precipitation (Qian et al., 2009; Liu et al., 2011; Wu et al., 2017). Through wavelet analysis, we found that light precipitation and LPAI were mainly concentrated in the 6 yr cycle.

We investigated factors affecting changes in light precipitation and found that temperature was the main influencing factor. According to previous research, most areas of the TP experienced a warming trend in recent decades. In the TP, surface temperature had increased by approximately 1.8℃ over the past 50 years (1960–2007), and the warming would have induced more precipitation in the eastern part of the TP (Liu and Chen, 2000). Some scholars have also pointed out that temperature affects changes in light precipitation (Qian et al., 2007; Wu et al., 2015). According to our correlation coefficients, other climatic factors had a small impact on micro–precipitation. In contrast, previous studies reported that these climatic factors have a greater impact on TP precipitation. The spatial distribution of precipitation anomalies in the TP and its adjacent areas was controlled by changes in the regional atmospheric circulation of the so-called 'plateau monsoon' on the decadal scale. ENSO may exert a direct impact on the East Asian summer monsoon precipitation by modulating the variability of the Philippine Sea anticyclone (Jin et al., 2018). NAO determines the spatial distribution of summer precipitation in the eastern part of the TP (Liu and Yin, 2001). Yang (2011) investigated relationships between AO and the precipitation and temperature over China, and found a good relationship between them over South China.

5 Conclusions

Our analysis revealed that the central and eastern TP mainly experienced light precipitation ($0.1 \leq Pre < 10.0$ mm/d) during 1961–2019. The amounts and days of light precipitation accounted for 30.7% and 81.5% of their corresponding total values. Therefore, light precipitation is a key indicator of central and eastern TP climate change. The amount and number of days of light precipitation exhibited increasing trends over the study period. We also found the same temporal and spatial characteristics for light precipitation events of various intensities (G1–G5 light precipitation). Light precipitation events gradually increased from the northwest to the southeast, and their intensity was higher in the southeast than in the northwest. The major cycle of G1–G5 light precipitation and LPAI over the study period was 6 yr with apparent periodic oscillation characteristics, and this cycle coexisted with cycles of other scales. A major abrupt change of light precipitation occurred in 1980, after which light precipitation mainly showed an increasing trend. We also observed that although G1 light precipitation accounted for only approximately 14% of the total amount of precipitation, the number of days of G1 light precipitation accounted for more than 40%. Therefore, we believe that G1 ($0.1 \leq Pre < 2.0$ mm/d) is more in line with the light precipitation standard for the central and eastern TP. In the future, when we study the light precipitation in central and eastern TP, we should pay more attention to G1 light precipitation. Analyzing G1 light precipitation will give us a clearer understanding of the causes of central and eastern TP climate change, and will be the key to our future research on the factors affecting the central and eastern TP drought and vegetation growth.

References

Anderegg W R L, Trugman A T, Badgley G et al., 2020. Divergen forest sensitivity to repeated extreme droughts. *Nat. Clim. Change*, 10: 1091–1095. doi: 10.1038/s41558-020-00919-1

Bett P E, Scaife A A, Li C F et al., 2018. Seasonal forecasts of the summer 2016 Yangtze River basin precipitation. *Advances in Atmospheric Sciences*, 35(8): 918–926. doi: 10.1007/s00376-018-7210-y

Bettolli, M L, Solman, S A, da Rocha, R P et al., 2021. The CORDEX flagship pilot study in southeastern South America: a comparative study of statistical and dynamical downscaling models in simulating daily extreme precipitation events. *Climate Dynamics*, 56(5): 1589–1608. doi: 10.1007/s00382-020-05549-z

Cao L G, Pan S M, 2014. Changes in precipitation extremes over the 'Three-River Headwaters' region, hinterland of the Tibetan Plateau, during 1960-2012. *Quaternary International*, 321: 105–115. doi: 10.1016/j.quaint.2013.12.041

Cao L G, Pan S M, Wang Q et al., 2014. Changes in extreme wet events in Southwestern China in 1960-2011. *Quaternary International*, 321: 116–124. doi: 10.1016/j.quaint.2013.11.014

Chen H P, Sun J Q, 2019. Increased population exposure to extreme droughts in China due to 0.5℃ of additional warming. *Environmental Research Letters*, 14(6): 064011. doi: 10.1088/1748–9326/ab072e

Cong Z Y, Kang S C, Liu X D et al., 2007. Elemental composition of aerosol in the Nam Co region, Tibetan Plateau, during

summer monsoon season. *Atmospheric Environment*, 41(6): 1180–1187. doi: 10.1016/j.atmosenv.2006.09.046

da Silva R M, Santos C A G, Moreira M et al., 2015. Rainfall and river flow trends using Mann-Kendall and Sen's slope estimator statistical tests in the Cobres River basin. *Natural Hazards*, 77(2): 1205–1221. doi: 10.1007/s11069-015-1644-7

da Silva R C, Mendes R M, Fisch G, et al., 2020. Future scenarios (2021–2050) of extreme precipitation events that trigger landslides—a case study of the Paraitinga River watershed, SP. *Brazil. Ambiente & Água*, 15(7): 1−18. doi:10.4136/ambi-agua.2558

Duan A M, Hu J, Xiao Z X, 2013. The Tibetan Plateau summer monsoon in the CMIP5 simulations. *Journal of Climate*, 26(19): 7747–7766. doi: 10.1175/JCLI-D-12-00685.1

Feng L, Zhou T J, 2012. Water vapor transport for summer precipitation over the Tibetan Plateau: Multidata set analysis. *Journal of Geophysical Research: Atmospheres*, 117: D20114. doi: 10.1029/2011JD017012

Fu C B, Dan L, 2014. Trends in the different grades of precipitation over South China during 1960-2010 and the possible link with anthropogenic aerosols. *Advances in Atmospheric Sciences*, 31(2): 480–491. doi: 10.1007/s00376-013-2102-7

Ge Sang, Tang Xiaoping, Lu Hongya, 2008. Climatic characteristics of rainfall and rainy days during the last 35 years over the Qinghai-Xizang Plateau. *Acta Geographica Sinica*, 63(9): 924–930. (in Chinese)

Gong D Y, Ho C H, Chen D L et al., 2007. Weekly cycle of aerosol - meteorology interaction over China. *Journal of Geophysical Research: Atmospheres*, 112: D22202. doi: 10.1029/2007JD008888

Grigholm B, Mayewski P A, Kang S et al., 2009. Atmospheric soluble dust records from a Tibetan ice core: possible climate proxies and teleconnection with the Pacific Decadal Oscillation. *Journal of Geophysical Research*, 114: D20118. doi: 10.1029/2008JD011242

Huang J P, Minnis P, Yi Y H et al., 2007. Summer dust aerosols detected from CALIPSO over the Tibetan Plateau. *Geophysical Research Letters*, 34: L18805. doi: 10.1029/2007GL029938

IPCC, 2013. *Climate Change 2013: The Physical Science Basic. Contribution of Working Group I to the Fifth Assessment Report of the Intergovernmental Panel on Climate Change.* Cambridge, United Kingdom and New York, USA: Cambridge University Press. available at http://www.climatechange2013.org/images/uploads/WGI.

Jiang Z H, Shen Y C, Ma T T et al., 2014. Changes of precipitation intensity spectra in different regions of mainland China during 1961-2006. *Journal of Meteorological Research*, 28(6): 1085–1098. doi: 10.1007/s13351-014-3233-1

Jin R, Wu Z W, Zhang P, 2018. Tibetan Plateau capacitor effect during the summer preceding ENSO: from the Yellow River climate perspective. *Climate Dynamics*, 51(1−2): 57–71. doi: 10.1007/s00382-017-3906-4

Kendall MG, Gibbons J D, 1981. *Rank correlation methods*, 5th. London, UK: Edward Arnold, 320.

Kidd C, Joe P, 2007. *Importance, identification and measurement of light precipitation at mid-to high-latitudes*. Proc. Joint EUMETSAT Meteorological Satellite Conf. and 15th Satellite Meteorology and Oceanography Conf.. Amsterdam, Netherlands: EUMETSAT and Amer. Meteor: 6.

Lau K M, Kim M K, Kim K M, 2006. Asian summer monsoon anomalies induced by aerosol direct forcing: the role of the Tibetan Plateau. *Climate Dynamics*, 26: 855–864. doi: 10.1007/s00382-006-0114-z

Li L C, Zou Y F, Li Y et al., 2020. Trends, change points and spatial variability in extreme precipitation events from 1961 to 2017 in China. *Hydrology Research*, 51(3): 484–504. doi: 10.2166/nh.2020.095

Li Y Q, Li D J, Yang S et al., 2010. Characteristics of the precipitation over the eastern edge of the Tibetan Plateau. *Meteorology and Atmospheric Physics*, 106(1-2): 49–56. doi: 10.1007/s00703-009-0048-1

Liang Liqiao, LI Lijuan, ZHANG Li et al., 2008. Sensitivity of Penman-Monteith reference crop evapotranspiration in Tao'er River Basin of northeastern China. *Chinese Geographical Science*, 18(4): 340–347. doi: 10.1007/s11769-008-0340-x

Liu B H, Xu M, Henderson M et al., 2005. Observed trends of precipitation amount, frequency, and intensity in China, 1960-2000. *Journal of Geophysical Research: Atmoshperes*, 110: D08103. doi: 10.1029/2004JD004864

Liu B H, Xu M, Henderson M, 2011. Where have all the showers gone? Regional declines in light precipitation events in China, 1960-2000. *International Journal of Climatology*, 31(8): 1177–1191. doi: 10.1002/joc.2144

Liu R, Liu S C, Cicerone R J et al., 2015. Trends of extreme precipitation in eastern China and their possible causes. *Advances in Atmospheric Sciences*, 32(8): 1027–1037. doi: 10.1007/s00376-015-5002-1

Liu X D, Chen B D, 2000. Climatic warming in the Tibetan Plateau during recent decades. *International Journal of Climatology*, 20(14): 1729–1742. doi: 10.1002/1097-0088(20001130)20:14<1729::AID-JOC556>3.0.CO;2-Y

Liu X D, Yin Z Y, 2001. Spatial and temporal variation of summer precipitation over the eastern Tibetan Plateau and the North Atlantic Oscillation. *Journal of Climate*, 14(13): 2896–2909. doi: 10.1175/1520-0442(2001)014<2896:SATVOS>2.0.CO;2

Mann H B, 1945. Nonparametric tests against trend. *Econometrica*, 13(3): 245–259. doi: 10.2307/1907187

Maussion F, Scherer D, Mölg T et al., 2014. Precipitation seasonality and variability over the Tibetan Plateau as resolved by the high asia reanalysis. *Journal of Climate*, 27(5): 1910–1927. doi: 10.1175/JCLI-D-13-00282.1

Ma S M, Zhou T J, Dai A G et al., 2015. Observed changes in the distributions of daily precipitation frequency and amount over China from 1960 to 2013. *Journal of Climate*, 28(17): 6960–6978. doi: 10.1175/JCLI-D-15-0011.1

Niu T, Chen L X, Zhou Z J, 2004. The characteristics of climate change over the Tibetan Plateau in the last 40 years and the de-

tection of climatic jumps. *Advances in Atmospheric Sciences*, 21(2): 193–203. doi: 10.1007/BF02915705

Pan T, Zhang L J, Zhang H W et al., 2020. Spatiotemporal patterns and variations of winter extreme precipitation over terrestrial northern hemisphere in the past century (1901−2017). *Physics and Chemistry of the Earth, Parts A/B/C*, 115: 102828. doi: 10.1016/j.pce.2019.102828

Qian W H, Fu J L, Yan Z W, 2007. Decrease of light rain events in summer associated with a warming environment in China during 1961−2005. *Geophysical Research Letters*, 34(11): L11705. doi: 10.1029/2007GL029631

Qian Y, Gong D Y, Fan J W et al., 2009. Heavy pollution suppresses light rain in China: observations and modeling. *Journal of Geophysical Research: Atmospheres*, 114(D7): D00K02. doi: 10.1029/2008JD011575

Qian Y, Gong D Y, Leung R, 2010. Light rain events change over North America, Europe, and Asia for 1973-2009. *Atmospheric Science Letters*, 11(4): 301–306. doi: 10.1002/asl.2980

Sen Roy S, Rouault M, 2013. Spatial patterns of seasonal scale trends in extreme hourly precipitation in South Africa. *Applied Geography*, 39: 151–157. doi: 10.1016/j.apgeog.2012.11.022

Shao L L, Tian L D, Cai Z Y et al., 2017. Driver of the interannual variations of isotope in ice core from the middle of Tibetan Plateau. *Atmospheric Research*, 188: 48–54. doi: 10.1016/j.atmosres.2017.01.006

Sun J, Yang K, Guo W D et al., 2020. Why has the inner Tibetan Plateau become wetter since the mid-1990s? *Journal of Climate*, 33(19): 8507–8522. doi: 10.1175/JCLI-D-19-0471.1

Tao S Y, Ding Y H, 1981. Observational evidence of the influence of the Qinghai-Xizang (Tibet) Plateau on the occurrence of heavy rain and severe convective storms in China. *Bulletin of the American Meteorological Society*, 62(1): 23–30. doi: 10.1175/1520-0477(1981)062<0023:OEOTIO>2.0.CO;2

Tao S Y, Zhang Q Y, Zhang S L, 1998. The influences of Tibetan plateau on weather anomalies over Changjiang River in 1998. *Acta Meteorologica Sinica*, 60(4): 3–5.

Tellman B, Sullivan J A, Kuhn C et al., 2021. Satellite imaging reveals increased proportion of population exposed to floods. *Nature*, 596(7080): 80–86. doi: 10.1038/s41586-021-03695-w

Thornthwaite C W, 1951. The water balance in tropical climates. *Bulletin of the American Meteorological Society*, 32: 166–173. doi: 10.1175/1520-0477-32.5.166

Tian G J, Qiao Z, Xu X L, 2014. Characteristics of particulate matter (PM10) and its relationship with meteorological factors during 2001 –2012 in Beijing. *Environmental Pollution*, 192: 266–274. doi: 10.1016/j.envpol.2014.04.036

Ueda H, Kamahori H, Yamazaki N, 2003. Seasonal contrasting features of heat and moisture budgets between the eastern and western Tibetan Plateau during the GAME IOP. *Journal of Climate*, 16(4): 2309–2324. doi: 10.1175/2757.1

Wang L Z, Cao L G, De ng, X J et al., 2014. Changes in aridity index and reference evapotranspiration over the central and eastern Tibetan Plateau in China during 1960-2012. *Quaternary International*, 349: 280–286. doi: 10.1016/j.quaint.2014.07.030

Wang J Z, Yang Y Q, Xu X D et al., 2003. A monitoring study of the 1998 rainstorm along the Yangtze River of China by using TIPEX data. *Advances in Atmospheric Sciences*, 20: 425–436. doi: 10.1007/BF02690800

Wang Y, Ma P L, Jiang J H et al., 2016. Toward reconciling the influence of atmospheric aerosols and greenhouse gases on light precipitation changes in Eastern China. *Journal of Geophysical Research: Atmospheres*, 121(10): 5878–5887. doi: 10.1002/2016JD024845

Wen G H, Huang G, Tao W C et al., 2016. Observed trends in light precipitation events over global land during 1961-2010. *Theoretical and Applied Climatology*, 125(1-2): 161–173. doi: 10.1007/s00704-015-1500-4

Wu G X, Zhang Y S, 1998. Tibetan Plateau forcing and the timing of the monsoon onset over south Asia and the South China Sea. *Monthly Weather Review*, 126(4): 913–927. doi: 10.1175/1520-0493(1998)126<0913:TPFATT>2.0.CO;2

Wu J, Ling C Y, Zhao D M et al., 2016. A counterexample of aerosol suppressing light rain in Southwest China during 1951-2011. *Atmospheric Science Letters*, 17(9): 487–491. doi: 10.1002/asl.682

Wu J, Zhang L Y, Zhao D M et al., 2015. Impacts of warming and water vapor content on the decrease in light rain days during the warm season over eastern China. *Climate Dynamics*, 45(7-8): 1841–1857. doi: 10.1007/s00382-014-2438-4

Wu J, Zhang L Y, Gao Y C et al., 2017. Impacts of cloud cover on long-term changes in light rain in Eastern China. *International Journal of Climatology*, 37: 4409–4416. doi: 10.1002/joc.5095

Xu Z X, Gong T L, Li J Y, 2008. Decadal trend of climate in the Tibetan Plateau-regional temperature and precipitation. *Hydrological Processes*, 22(16): 3056–3065. doi: 10.1002/hyp.6892

Yang H, 2011. The significant relationship between the Arctic Oscillation (AO) in December and the January climate over South China. *Advances in Atmospheric Sciences*, 28: 398–407. doi: 10.1007/s00376-010-0019-y

Yao T D, Thompson L, Yang W et al., 2012. Different glacier status with atmospheric circulations in Tibetan Plateau and surroundings. *Nature Climate Change*, 2: 663–667. doi: 10.1038/nclimate1580

You Q L, Kang S C, Pepin N et al., 2010. Climate warming and associated changes in atmospheric circulation in the eastern and central Tibetan Plateau from a homogenized dataset. *Global and Planetary Change*, 72(1−2): 11–24. doi: 10.1016/j.gloplacha.2010.04.003

Zhai P M, Sun A J, Ren F M et al., 1999. Changes of climate extremes in China. *Climatic Change*, 42(1): 203–218. doi: 10.1007/978-94-015-9265-9-13

Zhang D L, Huang J P, Guan X D et al., 2013. Long-term trends of precipitable water and precipitation over the Tibetan Plateau derived from satellite and surface measurements. *Journal of Quantitative Spectroscopy and Radiative Transfer*, 122: 64–71. doi: 10.1016/j.jqsrt.2012.11.028

Zhang K X, Qian X Q, Liu P X et al., 2017. Variation characteristics and influences of climate factors on aridity index and its association with AO and ENSO in northern China from 1961 to 2012. *Theoretical and Applied Climatology*, 130(1−2): 523–533. doi: 10.1007/s00704-016-1887-6

Zhang K X, Yao Y L, Qian X Q et al., 2019. Various characteristics of precipitation concentration index and its cause analysis in China between 1960 and 2016. *International Journal of Climatology*, 39: 4648–4658. doi: 10.1002/joc.6092

Zhang X L, Wang S J, Zhang J M et al., 2015. Temporal and spatial variability in precipitation trends in the Southeast Tibetan Plateau during 1961−2012. *Climate of the Past*, 11: 447–487. doi: 10.5194/cpd-11-447-2015

Zhang W X, Zhou T J, 2020. Increasing impacts from extreme precipitation on population over China with global warming. *Science Bulletin*, 65(3): 243–252. doi: 10.1016/j.scib.2019.12.002

Zhang Y Q, Liu C M, You Q L et al., 2019. Decrease in light precipitation events in Huai River Eco-economic Corridor, a climate transitional zone in eastern China. *Atmospheric Research*, 226: 240–254. doi: 10.1016/j.atmosres.2019.04.027

Zhao C S, Tie X X, Lin Y P, 2006. A possible positive feedback of reduction of precipitation and increase in aerosols over eastern central China. *Geophysical Research Letters*, 33(11): L11814. doi: 10.1029/2006GL025959

Zhao Y, Xu X D, Chen B et al., 2016. The upstream 'strong signals' of the water vapor transport over the Tibetan Plateau during a heavy rainfall event in the Yangtze River Basin. *Advances in Atmospheric Sciences*, 33: 1343–1350. doi: 10.1007/s00376-016-6118-7